Volume 7, Number 1 (February 2014) p. 100-137 • ISSN 1983-4195

REVISTA IBRACON DE ESTRUTURAS E MATERIAIS

IBRACON STRUCTURES AND MATERIALS JOURNAL

Simplified modelling of cracking and collapse process on frames and arches of reinforced concrete

Modelagem simplificada do processo de fissuração e colapso em pórticos e arcos de concreto armado

D. L. N. F. AMORIM [a]
davidnf@usp.br

S. P. B. PROENÇA [a]
persival@sc.usp.br

J. FLÓREZ-LÓPEZ [b]
iflorez@ula.ve

Abstract

The consistent simulation of progressive failure and structural collapse processes still is a problem of great interest for the engineering. Among theories which are somehow capable of model such class of problems, the continuum damage mechanics is the latest. However, one of the issues that still persist is when in the numerical simulations the structure begins to present the strain localisation phenomenon, with consequent dependence of the results on the mesh used. To solve this problem several so-called regularisation methods were developed. Nevertheless, despite effectiveness these methods can insert a significant degree of complexity on the numerical approaches. In this paper is proposed a simplified methodology to nonlinear structural analysis of frames and arches by means of the previous localisation of inelastic phenomena on hinges, located on the edges of the finite elements of frame and arch. Therefore it is possible to circumvent the mesh dependency and to reproduce satisfactorily real problems, as the examples of reinforced concrete structures gathered at the end of this article.

Keywords: frames, arches, reiforced concrete, lumped dissipation mechanics, localisation.

Resumo

A simulação consistente de processos de falha progressiva e colapso estrutural ainda é um problema aberto de grande interesse para a engenharia. Dentre as teorias que são capazes de modelar de alguma forma tal classe de problemas, a mecânica do dano contínuo é a mais recente. Entretanto, um dos gargalos que ainda persistem é quando nas simulações numéricas a estrutura passa a apresentar o fenômeno de localização de deformações, com consequente dependência dos resultados sobre a malha empregada. Para sanar este problema diversos métodos ditos de regularização foram desenvolvidos. Todavia, apesar de eficazes, estes métodos podem inserir um grau de complexidade significativo nas abordagens numéricas. Neste trabalho propõe-se uma metodologia simplificada para análise estrutural não linear de pórticos e arcos por meio da localização prévia dos fenômenos inelásticos em rótulas, posicionadas nas extremidades dos elementos finitos de barra e arco. Desta forma é possível contornar a dependência de malha e reproduzir de forma satisfatória problemas reais, como mostram os exemplos de estruturas de concreto armado reunidos no fim deste artigo.

Palavras-chave: póticos, arcos, concreto armado, teoria de dissipação concentrada, localização.

[a] *Departamento de Engenharia de Estruturas, Escola de Engenharia de São Carlos, Universidade de São Paulo, São Carlos, SP, Brasil;*
[b] *Departamento de Engenharia de Estruturas, Universidad de Los Andes, Mérida, Venezuela.*

Received: 20 Nov 2013 • Accepted: 25 Jan 2014 • Available Online: 13 Feb 2014

© 2014 IBRACON

1. Introduction

Continuum damage mechanics (see [1], for instance) is the latest among the major theories to describe the progressive deterioration process and structural failure. The main idea is based on the simple introduction of an internal variable which characterises the state of material deterioration. This variable, so-called damage, usually takes values among zero and one. Damage is introduced on constitutive laws by means of the effective stress concept combined to a strain equivalence hypothesis. The theory has been applied successfully on the local description of a wide variety of deterioration mechanisms.

The scientific activity in this area has been very significant and, currently, the theme has become one of the most important of continuum mechanics with applications in structural engineering, particularly. Since the first published papers in the mid-sixties of the last century, the number of works, conferences and specialised journals on the subject became huge. Despite of intense scientific activity, the number of practical applications of this theory is limited to a few regular cases, especially due to the conceptual complexity of strain softening responses implicit on constitutive models of continuous media with damage. Indeed, a consequence of the strain equivalence hypothesis is that the damage variable couples to both strains, penalising directly the elastic properties, and stresses, on the functions which control the yield and plastic hardening processes. This “parasite” character of the damage variable leads to a loss of fundamental mathematical properties of uniqueness and the problem becomes ill-posed. Consequently the analyses may have several solutions, causing no convergence of the finite elements responses with mesh refinement. That is essentially why the classic versions of the continuum damage theory are not adequate to practical applications in spite of its conceptual consistency. Therefore, the search for regularisation procedures of the mathematical damage models became a crucial task.

Initially the researchers sought for regularisation methods which may be used at any context or application. Among these, the most known and studied are the nonlocal damage models [2] and the similar ones so-called damage gradient models [3]. However, these approaches have not also been translated into more objective practical applications. Aside the mathematical aspects, the physical justifications of these models classes are limited and, numerically, the problems become overmuch complex for thinking in the resolution of real engineering problems, which require three-dimensional approaches.

An alternative to the regularisation processes consists on the development of simplified methods. This focus presents as main advantages: the well-posedness of mathematical problems, in most cases; the good understanding, or justification, of the simplified methods and the simple interpretation of the results. Finally, the computational effort is significantly reduced. One of the most used simplified methods consists in the utilisation of plastic, or inelastic, hinges coupled with damage. This combination gives place to theories of lumped damage mechanics (LDM). Such approach has been successfully used to modelling reinforced concrete (RC) [4-12] or steel frames [13]. The damage hinges may be used to modelling the concrete cracking in reinforced concrete structures, and local buckling in tubular steel structures.

So far the LDM has been considered only by straight frame elements. However, RC arches and rings are also important structural alternatives, compounding, among other applications, tunnels ceiling reinforcements and several structures employed on hydraulic and sanitation. In terms of finite element method applications, the formulation of bar elements with curve axis is not new. An especial finite element for elastic circular arches was proposed in [14]. This research was extended to parabolic frames [15]. Most recently, it was proposed another circular arch element with plastic hinges [16]. Notwithstanding, neither of these studies consider the phenomena associated to concrete cracking.

In fact, the dominant failure mechanism in tunnels, conducts and arches is precisely the concrete fracture when the instabilities are controlled. Broadly speaking, there are two alternatives for modelling cracking phenomena. The first one is based on the using of classic continuum damage theory in combination with beam, shell or solid finite elements (see e.g. [17]), exploring regularisation of localisation issues aforementioned. The second one consists on the using of fracture mechanics [18]. However, the inclusion of reinforcement effects on the crack propagation and the computational fracture mechanics complexity itself render this approach really difficult for practical applications.

In this work a general theory based on LDM to analyse general purpose curvilinear structures is presented. This generalisation of the theory arises from combining methods of LDM and procedures presented in [14,16]. In this way, a very efficient numerical procedure for structural analyses is achieved, using few elements, with good precision and consistently accounting for the strain softening response, therefore, including all necessary information for a representative evaluation. Hopefully, this approach may be useful in practical terms, hence constituting itself into an interesting alternative to subsidise real structural engineering projects.

This paper is organised as follows: in the first two subsequent sections a general theory of inelastic frames behaviour is described. The notation introduced in [19] is adopted, which is considered more appropriate in case of complex constitutive laws. In the next four sections the proposed model is described. Then, a procedure for numerical implementation within conventional finite element codes is presented. Finally, the performance of the proposed model is illustrated by means of two numerical simulations.

2. Static of structures composed by straight and circular elements

Consider a plain frame composed by straight and circular elements, as indicated in figure 1. According to a global reference system $X_G Z_G$, generalised displacements of a frame node i are represented by: u_i, w_i, θ_i and external forces on the node j are: $P_{uj} P_{wj} P_{\theta j}$. The vector of external nodal forces of a structure with n nodes is indicated as:

$$\{\mathbf{P}\}^t = (P_{u1}, P_{w1}, P_{\theta 1}, P_{u2}, ..., P_{wn}, P_{\theta n}) \quad (1)$$

Consider now a frame element b, straight or circular, defined between nodes i and j. Straight elements are characterised by nodal coordinates on the global system, while circular elements, besides that, also need the radius R_b. The vector of internal nodal forces generated by the element b is indicated as:

Figure 1 – External forces and generalised displacements according to the global reference system

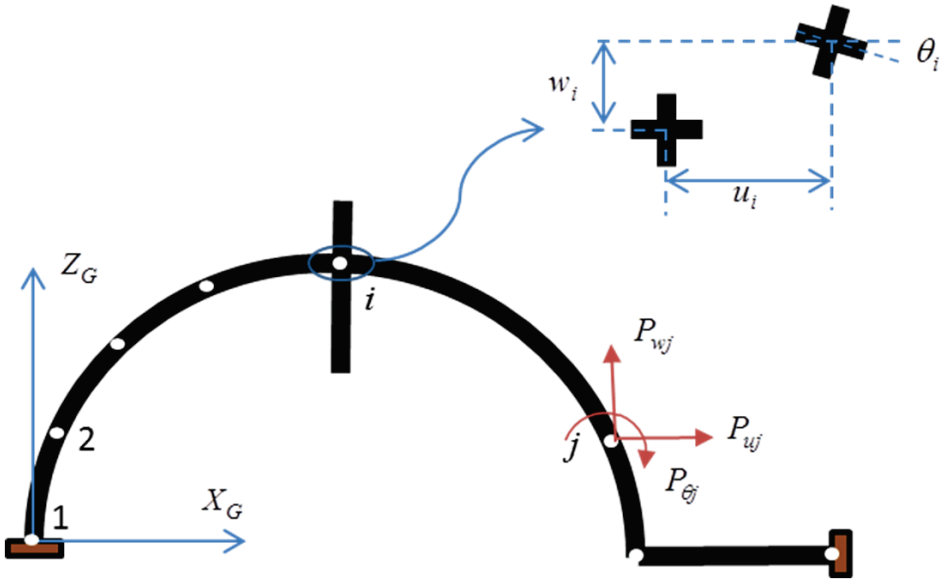

$$\{\mathbf{Q}\}_b^t = (Q_{ui}, Q_{wi}, Q_{\theta i}, Q_{uj}, Q_{wj}, Q_{\theta j}) \quad (2)$$

It follows that the quasi-static equilibrium equations may be written as:

$$\sum_b \{\mathbf{Q}_A\}_b = \{\mathbf{P}\} \quad (3)$$

where, by consistency with the dimensional order of each part of the sum, the internal force matrices $\{\mathbf{Q}_A\}_b$ are expanded by including zeros on degrees of freedom not correspondent to the element nodes:

$$\{\mathbf{Q}_A\}_b^t = (\underbrace{0,0,0}_{\text{nó } 1},\ldots,\underbrace{Q_{ui}, Q_{wi}, Q_{\theta i}}_{\text{nó } i},\underbrace{0,0,0}_{\text{nó } i+1},\ldots,\underbrace{Q_{uj}, Q_{wj}, Q_{\theta j}}_{\text{nó } j},\underbrace{0,0,0}_{\text{nó } j+1},\ldots) \quad (4)$$

For each element is introduced a local reference system $x_b z_b$, as illustrated in figure 2. In straight elements the local origin coincides with node i and the x_b axis aligns with the chord i–j. The angle between the

Figure 2 – Local reference systems

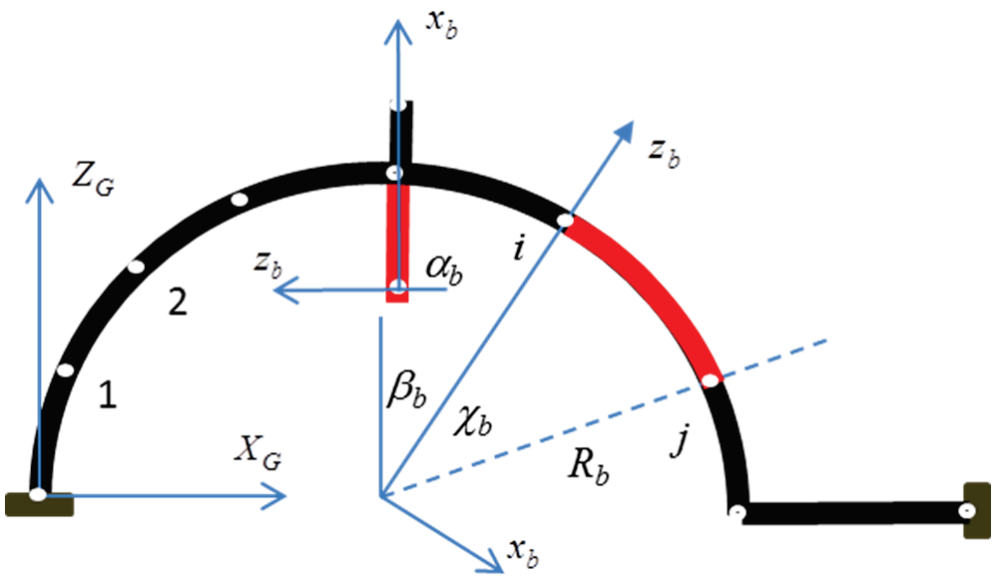

Figure 3 – Internal forces and generalised stresses on the: (a) straight and (b) curved element

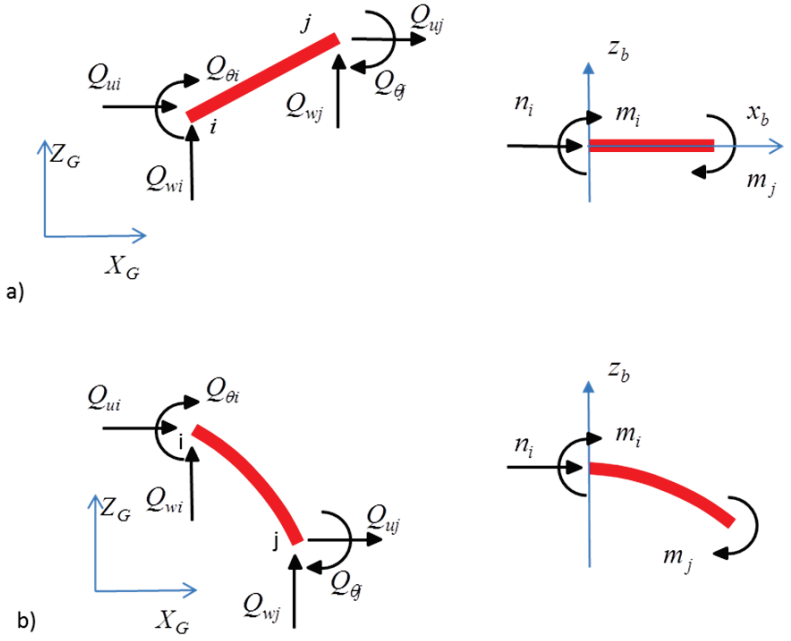

local x_b and global X_G axes is represented by a_b. Naturally the angle a_b and the length L_b may be calculated by means of the nodes i and j according to the global system. In case of circular elements the origin of the system is placed in the centre of arch, the axis z_b passes thru node i and β_b is the angle between the global Z_G and local axes z_b. The element forms a circle arch c_b. The angles b_b and c_b may also be calculated by means of the nodes and element radius, as shown in appendix 1.

Using the same approach of [19] to a nonlinear elastic frame analysis, it is defined a second set of static variables coupled up to local reference: the generalised stress vector of the element (see figure 3):

$$\{\boldsymbol{\sigma}\}_b^t = (m_i, m_j, n_i) \tag{5}$$

On the generalised stress vector, m_i and m_j are the bending moments on sections i and j, respectively, and n_i is the axial force (positive compression) in i. The vectors of internal forces and stress are related by means of the following equation of static equilibrium:

$$\{\mathbf{Q}\} = [\mathbf{B}]_b^t \{\boldsymbol{\sigma}\}_b \tag{6}$$

where $[\mathbf{B}]_b$ is called kinematic transformation matrix of the element b. The determination of the matrix $[\mathbf{B}]_b$ to straight and curved elements is indicated in the appendix 2.

The matrix of external forces also may be related to generalised stresses combining equations (3,6):

$$\sum_b [\mathbf{B}_A]_b^t \{\boldsymbol{\sigma}\}_b = \{\mathbf{P}\} \tag{7}$$

where the expanded kinematic transformation matrix $[\mathbf{B}_A]_b^t$ is built in a similar way as indicated in equation (4).

3. Kinematic of structures including straight and circular elements

The nodal generalised displacement vectors of a frame and the analogous vector of an element b between nodes i and j are, respectively:

$$\{\mathbf{U}\}^t = (u_1, w_1, \theta_1, u_2, \ldots\ldots, w_n, \theta_n) \quad \{\mathbf{q}\}_b^t = (u_i, w_i, \theta_i, u_j, w_j, \theta_j) \tag{8}$$

At the element level an additional kinematic variable is defined, which is called generalised deformation matrix $\{\varepsilon\}_b$, being conjugated with generalised stresses by means of the mechanical potency $\dot{W}_b$:

$$\dot{W}_b = \{\dot{\boldsymbol{\varepsilon}}\}_b^t \{\boldsymbol{\sigma}\}_b = \{\dot{\mathbf{q}}\}_b^t \{\mathbf{Q}\}_b \tag{9}$$

On the other hand, the generalised deformations may be calculated through nodal generalised displacements of the element. Actually, combining equations (6-9) the following relation can be obtained:

$$\left(\{\dot{\boldsymbol{\varepsilon}}\}_b^t - \{\dot{\mathbf{q}}\}_b^t [\mathbf{B}]_b^t\right)\{\boldsymbol{\sigma}\}_b = 0 \quad \forall \{\boldsymbol{\sigma}\}_b \quad \text{i.e.} \quad \{\dot{\boldsymbol{\varepsilon}}\}_b = [\mathbf{B}]_b \{\dot{\mathbf{q}}\}_b \tag{10}$$

The deformation rates of the element also may be expressed in

terms of the nodal displacement rates of the frame, using the expanded transformations matrix:

$$\{\dot{\varepsilon}\}_b = [\mathbf{B}_A]_b \{\dot{\mathbf{U}}\} \quad (11)$$

In case of small displacements, the transformation matrices related to the initial $[\mathbf{B}_o]_b$ and deformed $[\mathbf{B}]_b$ configurations are practically the same [19]:

$$[\mathbf{B}]_b \cong [\mathbf{B}_o]_b \quad (12)$$

Then the kinematic and static equilibrium equations may be written as:

$$\{\boldsymbol{\varepsilon}\}_b = [\mathbf{B}_{oA}]_b \{\mathbf{U}\} \quad (13)\,a$$

$$\{\mathbf{Q}\}_b = [\mathbf{B}_o]_b^t \{\boldsymbol{\sigma}\}_b \quad (13)\,b$$

4. Hypothesis of strain equivalence and lumped dissipation

On the classical theory of continuum damage (see e.g. [1]) the degradation process of mechanical properties of the solid is represented by means of a variable called continuum damage ω which can take values between zero and one. The continuum damage is introduced in elastic constitutive law using the effective stress concept (that occurs on the undamaged part with defects) and the strain equivalence hypothesis (the undamaged part submitted to effective stress presents same strain that the degraded part on nominal stress):

$$\bar{\sigma} = \frac{\sigma}{1-\omega} \qquad \bar{\sigma} = E(\varepsilon - \varepsilon^p) \Rightarrow \sigma = (1-\omega)E(\varepsilon - \varepsilon^p) \quad (14)$$

being σ the Cauchy stress, or nominal stress in case of small strains, $\bar{\sigma}$ the effective stress, E the Young's Modulus, ε the total strain and ε^p the portion of plastic strain.

The elastic constitutive relation (14) may be written also in terms of flexibility [9]. This alternative implies the following relations:

$$\varepsilon - \varepsilon^p = \frac{1}{(1-\omega)E}\sigma \Rightarrow \varepsilon = \varepsilon^e + \varepsilon^d + \varepsilon^p$$

$$\varepsilon^e = \frac{1}{E}\sigma \qquad \varepsilon^d = \frac{\omega}{E(1-\omega)}\sigma \quad (15)$$

The specific strain can be decomposed in three parts: an elastic term calculated by Hooke's law, a plastic and damage terms, which arises from micro-defects accumulation on material. This last term of strain is null if there is no damage and tends to an infinite value when the damage tends to one. From equations (15) also provide the interpretation that the material has an initial elastic flexibility $1/E$ and an additional flexibility due to material deterioration expressed by: $\omega/E(1-\omega)$. Naturally, the additional flexibility does not exist when the material presents no damage and tends to infinite when the damage tends to one.

To take into account in a simplified way the inelastic effects of plasticity and damage on frame problems, it is assumed the hypothesis of lumped dissipation. Such hypothesis assumes that all inelastic effects are concentrated in plastic hinges (with zero-length) with damage. Therefore, it is supposed that a frame element combines an elastic component and two inelastic hinges localised at its edges (see figure 4).

The application of the strain equivalence hypothesis in this context leads to the following expression:

$$\{\boldsymbol{\varepsilon}\}_b = \{\boldsymbol{\varepsilon}^e\}_b + \{\boldsymbol{\varepsilon}^p\}_b + \{\boldsymbol{\varepsilon}^d\}_b \quad (16)$$

The matrix $\{\varepsilon^e\}_b$ contains the elastic generalised strain components of the element. These strains are expressed in terms of the generalised stresses, using the elastic flexibility matrix $[\mathbf{F}_o]$:

$$\{\boldsymbol{\varepsilon}^e\}_b = [\mathbf{F}_o]\{\boldsymbol{\sigma}\}_b \quad (17)$$

Figure 4 – Lumped dissipation model a) straight element b) curved element

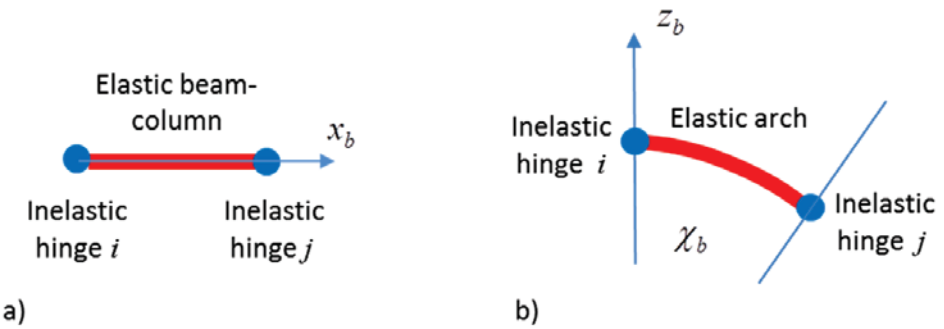

Figure 5 – Plastic elongation and rotations

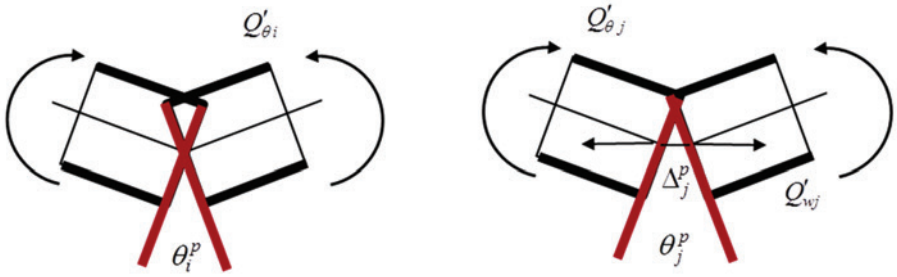

Hinge *i* and pure bending | Hinge *j* and bending with traction

The expressions of $[\mathbf{F}_o]$ are presented in appendix 3.

5. Internal variables: plastic rotations and damage on hinges

The hinges may have plastic rotations and elongations as indicated in figure 5. Therefore, the plastic dissipated energy of the element is [16]:

$$\dot{W}_p = Q'_{\theta i}\dot{\theta}_i^p - Q'_{ui}\dot{\Delta}_i^p + Q'_{\theta j}\dot{\theta}_j^p + Q'_{uj}\dot{\Delta}_j^p \quad (18)$$

where $Q'_{\theta i}, Q'_{ui}, Q'_{\theta j}, Q'_{uj}$ are the bending moments and axial forces on i and j element edges, as indicated in appendix 2.

On the other hand, be $\{\boldsymbol{\varepsilon}^p\}_\epsilon^t = (\phi_i^p, \phi_j^p, \delta^p)$ the components of generalised plastic strains matrix, then the plastic dissipation may also be written as:

$$\dot{W}_p = \{\boldsymbol{\varepsilon}^p\}_\epsilon^t \{\boldsymbol{\sigma}\} = m_i\dot{\phi}_i^p + m_j\dot{\phi}_j^p + n_i\dot{\delta}^p = Q'_{\theta i}\dot{\theta}_i^p - Q'_{ui}\dot{\Delta}_i^p + Q'_{\theta j}\dot{\theta}_j^p + Q'_{uj}\dot{\Delta}_j^p \quad (19)$$

In case of a straight element: $Q'_{\theta i} = m_i$, $Q'_{\theta j} = m_j$, $Q'_{uj} = -n_i$ and $Q'_{ui} = -n_i$. Thus, from relation (19) some physical interpretation to components of plastic strains matrix arise:

$$\phi_i^p = \theta_i^p \qquad \phi_j^p = \theta_j^p \qquad \delta^p = -(\Delta_i^p + \Delta_j^p) \quad (20)$$

i.e. the terms ϕ_i^p and ϕ_j^p are plastic rotations on hinges i and j, and δ^p is the permanent elongation of the element.

In case of a circular element we have: $Q'_{\theta i} = m_i$, $Q'_{\theta j} = m_j$, $Q'_{ui} = n_i$, $Q'_{uj} = -(m_i + nR + m_j)/R$ (see equation (2) of appendix 3), ergo:

$$\phi_i^p = \theta_i^p - \frac{\Delta_i^p}{R} \qquad \phi_j^p = \theta_j^p - \frac{\Delta_j^p}{R} \qquad \delta^p = -(\Delta_i^p + \Delta_j^p) \quad (21)$$

Thereby ϕ_i^p and ϕ_j^p are not exactly plastic rotations. However, to arches with large radius and small permanent elongations this difference is negligible, being possible to admit that ϕ_i^p and ϕ_j^p are plastic rotations.

Now, a second set of internal variables on hinges is introduced, gathered in the following damage vector: $\{\mathbf{D}\}_b^t = (d_i, d_j)$. These variables take values between zero and one, as in the case of continuum damage, however in the present model those variables measure densities of macro-cracking on concrete (see figure 6).

Thereby, according to the strain equivalence hypothesis the strains due to damage on hinges may be expressed as:

$$\{\boldsymbol{\varepsilon}^d\}_b = [\mathbf{C}(\mathbf{D})]\{\boldsymbol{\sigma}\}_b \quad [\mathbf{C}(\mathbf{D})] = \begin{bmatrix} \frac{d_i F_{11}^0}{(1-d_i)} & 0 & 0 \\ 0 & \frac{d_j F_{22}^0}{(1-d_j)} & 0 \\ 0 & 0 & 0 \end{bmatrix} \quad (22)$$

where F_{ij}^0 are coefficients of the elastic flexibility matrix of element. The equations (16, 17 and 22) allow writing the elasticity law of an element as:

$$\{\boldsymbol{\varepsilon} - \boldsymbol{\varepsilon}^p\}_b = [\mathbf{F}(\mathbf{D})]\{\boldsymbol{\sigma}\}_b \quad [\mathbf{F}(\mathbf{D})] = [\mathbf{F}_0] + [\mathbf{C}(\mathbf{D})] = \begin{bmatrix} \frac{F_{11}^0}{(1-d_i)} & F_{12}^0 & F_{13}^0 \\ F_{21}^0 & \frac{F_{22}^0}{(1-d_j)} & F_{23}^0 \\ F_{31}^0 & F_{32}^0 & F_{33}^0 \end{bmatrix} \quad (23)$$

The previous relation also evidences that the flexibility matrix of the element may be decomposed in an initial elastic term and an additional term due to damage. When the damage is zero the additional part of flexibility is null, since when the damage approaches the unit value the additional flexibility tends to infinity.

Figure 6 – Lumped damage variables on a straight element (4)

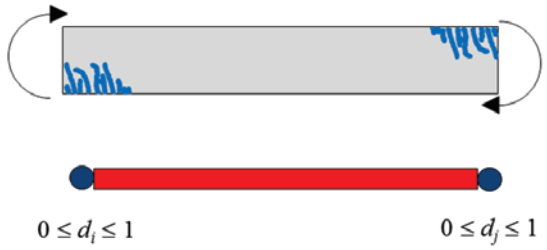

5.1 Generalised Griffith criterion for the calculation of damage in an inelastic hinge

On the classic Fracture Mechanics the criterion of crack propagation in a continuous environment is obtained from a balance of energy and introducing the energy release rate concept. An analogous approach may be conducted in the case of a frame element [4]. The complementary strain energy W_b of the element is:

$$W_b = \frac{1}{2}\{\boldsymbol{\sigma}\}_b^t\{\boldsymbol{\varepsilon}-\boldsymbol{\varepsilon}^p\}_b = \frac{1}{2}\{\boldsymbol{\sigma}\}_b^t[\mathbf{F}(\mathbf{D})]\{\boldsymbol{\sigma}\}_b \quad (24)$$

Then, the energy release rate of inelastic hinges is given by:

$$G_i = \frac{\partial W_b}{\partial d_i} = \frac{m_i^2 F_{11}^0}{2(1-d_i)^2} \qquad G_j = \frac{\partial W_b}{\partial d_j} = \frac{m_j^2 F_{22}^0}{2(1-d_j)^2} \quad (25)$$

In this case, the energy release rate acts as a crack inductor thermodynamic 'moment'. Hence, the Griffith criterion establishes that the propagation of damage in a hinge i is possible only if the inductor moment equate crack resistance $R(d_i)$. Once such critical condition is verified, the damage evolution, for each element, is governed by the following conditions:

$$\begin{cases} \Delta d_i > 0 & \Rightarrow \quad G_i = R(d_i) \\ G_i < R(d_i) & \Rightarrow \quad \Delta d_i = 0 \end{cases} \qquad \begin{cases} \Delta d_j > 0 & \Rightarrow \quad G_j = R(d_j) \\ G_j < R(d_j) & \Rightarrow \quad \Delta d_j = 0 \end{cases} \quad (26)$$

where Δd_i and Δd_j represent the damage increments on hinges i and j, respectively.

A relation to the crack resistance was proposed in [4] based on an experimental evaluation as:

$$R(d_i) = R_0 + q\frac{\ln(1-d_i)}{(1-d_i)} \quad (27)$$

The element has an initial crack resistance R_0 and a logarithmic hardening term proportional to parameter q. This last parameter accounts for the reinforcement effect in concrete, which hampers the crack propagation. The Griffith propagation condition, $G_i = R(d_i)$, describes, essentially, the relation between the bending moment on the hinge and the damage level, as illustrated in figure 7.

Figure 7 – Damage vs. bending moment on an inelastic hinge

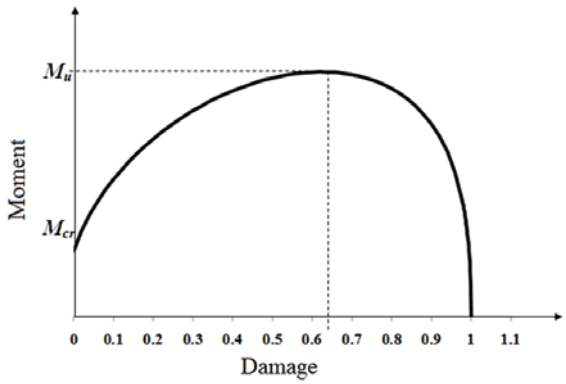

The parameters R_0 and q may be identified such that the damage-bending moment curve fits through points corresponding to the cracking moment of the cross-section M_{cr} and to the ultimate moment M_u [4]. This alternative allows dismissing experimental analysis for purposes of parametric identification, involving, therefore, only parameters and classical concepts of conventional reinforced concrete theory.

5.2 Evolution law of plastic rotation on a damaged hinge

The last set of equations of the simplified model is the evolution law of plastic strains. In the classic plasticity theory this relation is obtained from a yield function. In the simplified model two functions are introduced: $f_i \le 0$ and $f_j \le 0$, in correspondence to each inelastic hinge of the element. Being the hardening effect described by a kinematic model the aforementioned functions are given by:

$$f_i = \left|m_i^b - c\phi_i^p\right| - M_y \le 0; \qquad f_j = \left|m_j^b - c\phi_j^p\right| - M_y \le 0 \quad (28)$$

being M_y the effective plastic yield moment and c the effective plastic stiffness. Both parameters also may be calculated using the reinforced concrete theory [4].

Neglecting plastic elongations, the evolution laws of plastic rotations result from a complementary condition with the yield functions:

$$\begin{cases} \Delta\phi_i^p \ne 0 & \Rightarrow \quad f_i = 0 \\ f_i < 0 & \Rightarrow \quad \Delta\phi_i^p = 0 \end{cases} \qquad \begin{cases} \Delta\phi_j^p \ne 0 & \Rightarrow \quad f_j = 0 \\ f_j < 0 & \Rightarrow \quad \Delta\phi_j^p = 0 \end{cases} \quad (29)$$

To take into account also the effects of cracking moment, the yield functions may be modified using, again, the strain equivalence hypothesis in stiffness terms. Therefore, the effective moments $\overline{m}_i^b$ and $\overline{m}_b^b$ at hinges are defined as follows:

$$\overline{m}_i^b = \frac{m_i^b}{1-d_i} \qquad \overline{m}_j^b = \frac{m_j^b}{1-d_j} \tag{30}$$

Therewith, the yield functions with linear kinematic hardening can be rewritten as:

$$f_i = \left|\overline{m}_i^b - c\phi_i^p\right| - M_y = \left|\frac{m_i^b}{1-d_i} - c\phi_i^p\right| - M_y \leq 0$$
$$f_j = \left|\frac{m_j^b}{1-d_j} - c\phi_j^p\right| - M_y \leq 0 \tag{31}$$

6. Numerical implementation

Consider, again, the equilibrium equation (3) conveniently rewritten:

$$\{\mathbf{Res}\} = \sum_b \{\mathbf{Q}_A(\mathbf{U})\}_b - \{\mathbf{P}\} = 0 \tag{32}$$

Equation (32) establishes that the solution is only obtained when the residual force vector $\{\mathbf{Res}\}$, defined as the difference between the internal and external forces, is null.

A finite element programme is here composed of a set of routines that process the user input, generate the structure calculation process step-by-step and provide the analysis results in tabulated or graphical form. At each calculation step, the programme solves numerically the problem defined by the matrix equation (32) accounting for the boundary conditions. These conditions are defined by known displacement values in regions where the forces are unknown and vice-versa.

The finite element is fundamentally inserted in the routine that calculates the internal forces $\{\mathbf{Q}\}_b$ from displacements. The computational procedure that expands the matrices of internal forces and combines them in the matrix of residual forces is the well-known assemblage algorithm.

The proposed frame element is then defined by the kinematic equation (13a), which allows the strain calculation from displacements, by the elastic (23), damage (26) and plasticity (28) laws, which provide the generalised stresses and internal variables from strains and, finally, by the equilibrium equation (13b), which returns the internal forces from stresses.

The system of global equilibrium equations of the structure (31) is, in general, nonlinear. Therefore such system must be solved by linearization of the problem with some iterative method to correct the solution estimative, being the Newton's method or any of its variants usually employed. In this case, due to the linearization, it is also necessary the calculation of tangent stiffness matrix, or jacobian, of internal forces: $\left[\frac{\partial \mathbf{Q}(\mathbf{U})}{\partial \mathbf{U}}\right]_b$.

Notice that the constitutive model, represented by the set of equations (23,26,28) is also nonlinear. Therefore, it is necessary the use of Newton's method combined with a predictor and corrector strategy in local character. It is noteworthy that an especial characteristic of this type of local problem is that the convergence conditions vary significantly with the damage i.e. as higher the damage value to be calculated as lower is the increment size. Furthermore, loading increases are usually followed by damage concentration on few hinges. That is why the classical procedure, which involves calculations of both global and local equilibrium problems is not efficient. In this case, it is preferable to use different steps of calculation on each element [20]. Figure 8 shows a possible algorithm based on this idea.

7. Examples

7.1 Precast tunnel segment

In [21] experimental tests on precast segments that compose the Brennero Base Tunnel, which connects Italy to Austria are described. The tunnel is composed by six segments, presenting 19m of circumferential length and 6 m of external diameter. The considered segment presents dimensions of thickness, length and width equal to 200 mm, 3640 mm and 1500 mm, respectively (see figure 9).

The precast segment analysed in [21] presents concrete with characteristic compression strength of 50 MPa and flexural reinforcement composed by rebars with 8 mm of diameter (see figure 10).

Attempting to assess the response of the proposed model, the flexural test on the segment was hereby chosen (figure 11), among the described tests in [21].

Thus, taking advantage of symmetry of the problem, the simulation was realised using only two arch finite elements (figure 12).

In possession of the adopted material properties and of the cross-section characteristics [21], by using the classical theory of reinforced concrete interaction diagrams between axial force and bending moment in the section were obtained (figure 13). As the axial force along longitudinal direction of the tunnel structure may be neglected, from the interaction diagrams were identified values of 451 tf.cm, 550 tf.cm and 916 tf.cm to the cracking, plastic and ultimate moments, respectively.

The comparison between the numerical and experimental responses, in terms of load versus displacement of the point of load application, is presented in figure 14.

It is observed that the numerical solution is well fitted to the experimental response.

7.2 Prestressed and precast concrete segmental lining

To build a tunnel (figure 15a) in the city of Osaka [22], Japan, precast concrete segmental lining was used (figure 15b).

To analyse the structural behaviour were realised flexural tests (figure 16) on specimens composed by two precast segments, applying prestress force of 29.4 kN per strand, [22]. In experimental set the semi-circumference formed by the abovementioned assemblage was simply supported at the base, being the load applied in two points equidistant 450 mm of the central section of (see figure 17).

The numerical simulation was performed taken profit of the symmetry presented by the problem (figure 18).

The obtained response with the proposed model (figure 19) was compared to the average experimental response, given in [22]. It is noteworthy that the model parameters for this problem were experimentally measured, also considering the applied prestress.

It is observed that the proposed model can follow, satisfactorily, the

Figure 8 – Multistep algorithm

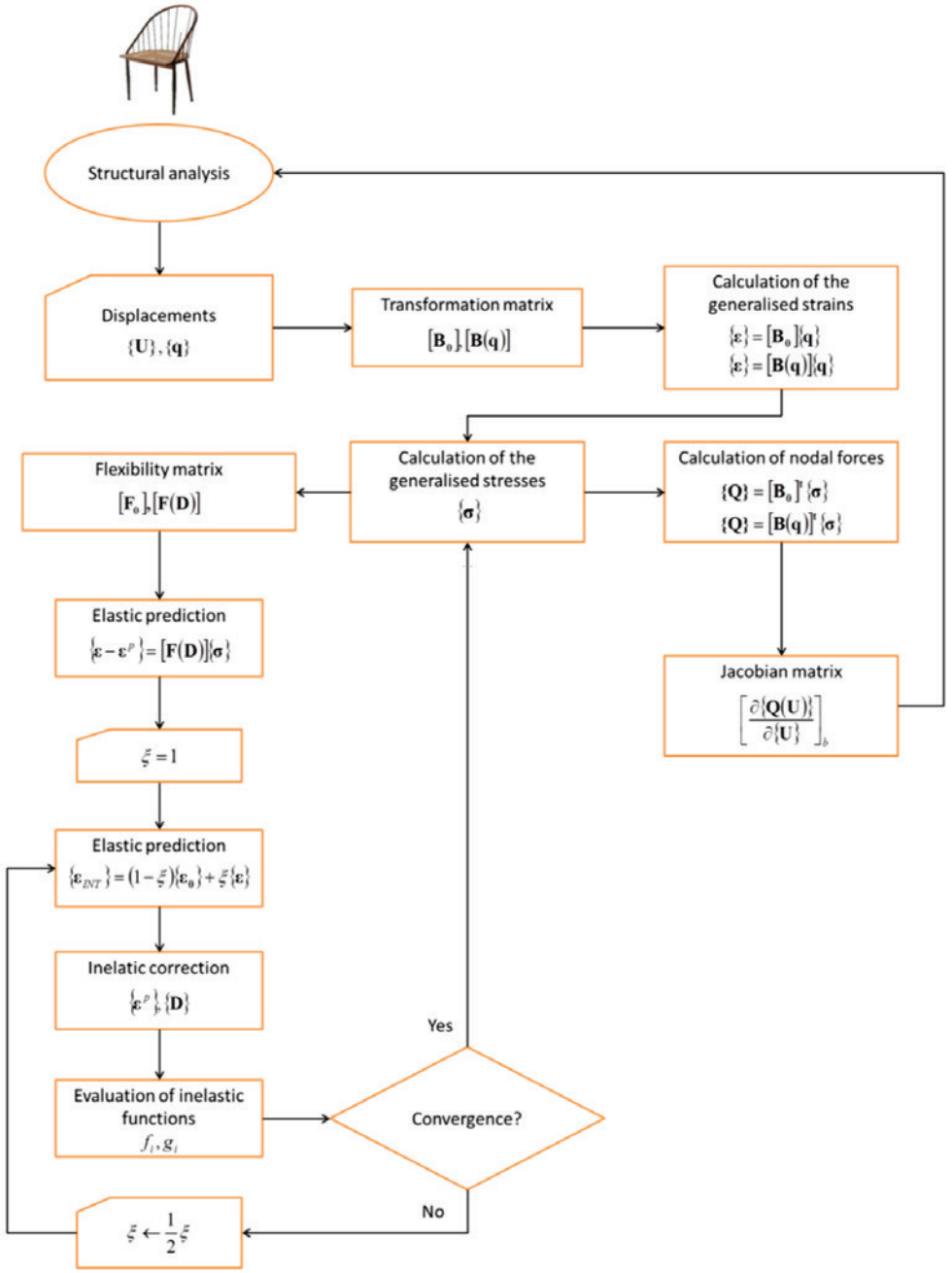

average experimental response, including its descendent stretch. This stretch occurs due to localisation phenomena of the inelastic effects in the region under the applied load. In the proposed model, this localised effect was captured on one of the inelastic hinges (figure 20a), to where the damage evolutions (figure 20b) and plastic rotations clearly converge, reaching concerning values related to the structural integrity.

Figure 21 overlaps the graphics presented in figures 19 and 20b, for a better analysis.

In figure 21 it is observed that the damage on hinges evolves quickly in the first stage of loading, being concrete cracking the only inelastic effect present. As soon as the reinforcement initiates its yielding process the damage growth turns less accelerated. At the instant that the structure reaches the maximum value of load resistance measured experimentally (see [22]), the damage on hinge '2' presents itself with intensity about 0.6, which is considered excessive to reinforced concrete structures, [23]. From this point on, the structure continues to deform in a process of controlled displacement. The damage responses, and also the plastic strain, keep constant at hinges '1' and '3'. However, the damage (and also the plastic strain) continues to evolve in hinge '2'. Thus, it is possible to affirm that beyond this point of the analysis the localisation phenomenon of inelastic processes occurs. It is noteworthy that the hinge '4' has not activated its inelastic processes throughout the analysis.

Figure 9 – Tunnel segment geometry (21)

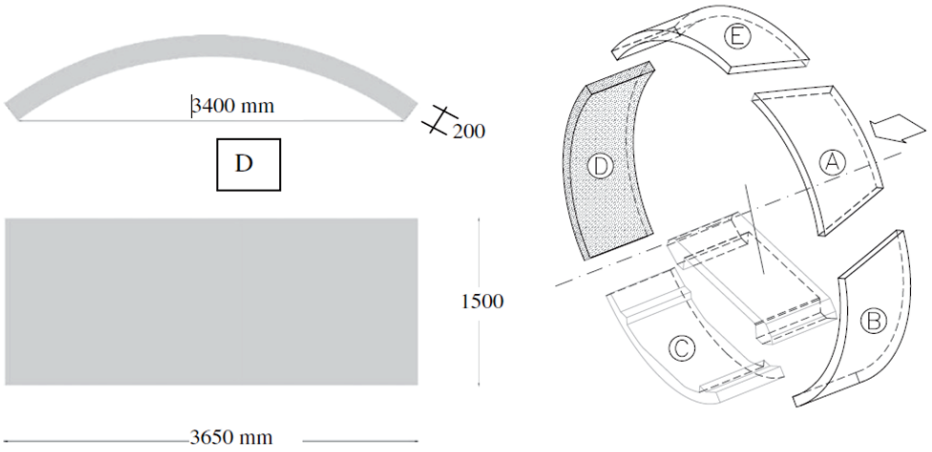

Figure 10 – Tunnel segment reinforcement (21)

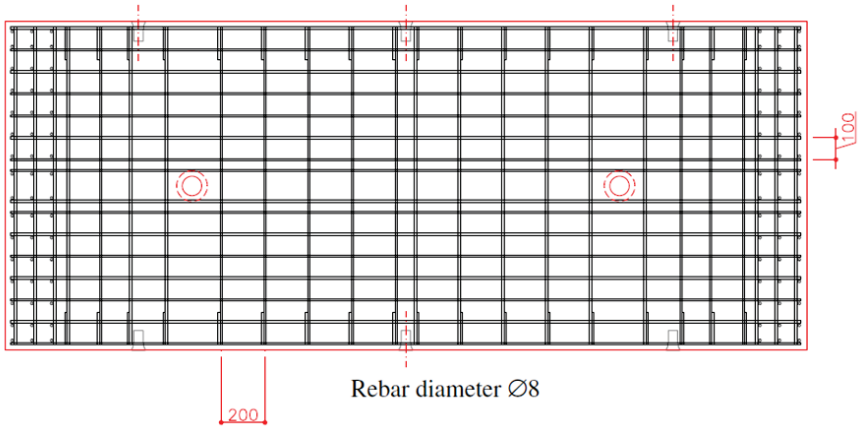

8. Conclusions

The formulation proposed in this paper aims to describe with good precision the behaviour of framed structures in presence of inelastic effects concentration. To assess the numerical response of the model two experimental tests of structures composed by circular arches were considered. In the first example, beyond the accuracy aspects, the robustness of the proposed formulation was put into test in a certain sense, since the parameters were obtained by using conventional theory of reinforced concrete. In the second example, it was observed that the formulation is also capable to reproduce, in a satisfactorily way, the localisation phenomenona of inelastic processes. Thus, it became clear that the proposed model is able to reproduce, consistently, nonlinear behaviour of real reinforced concrete structures.

9. References

[01] Lemaitre, J., Chaboche, J. L. Mechanics of Solids Materials, Dunod, Paris, 1988.

[02] Bazant, Z. P., Jirasek, M. Nonlocal Integral Formulations of Plasticity and Damage: Survey of Progress. Journal of Engineering Mechanics, v.128, n.11, 2002; p.1119–1149.

[03] Peerlings, R. H. J., de Borst, R., Brekelmans, W. A. M., de Vree, J. H. P. Gradient enhanced damage for quasi-brittle materials. International Journal for Numerical Methods in Engineering, v.39, n.19, 1996; p.3391–3403.

[04] A. Cipollina, A. López-Inojosa, J. Flórez-López, A simplified damage mechanics approach to nonlinear analysis of frames. Computers and Structures; v.54, n.6, 1995; p.1113-1126.

[05] M.E. Perdomo, A. Ramirez, J. Flórez-López, Simulation of damage in RC frames with variable axial forces. Earthquake Engineering and Structural Dynamics, v.28, n.3, 1999; p.311-328.

[06] Álvares, M. S. Contribuição ao estudo e emprego de modelos simplificados de dano e plasticidade para a análise de estruturas de barras em concreto armado, São Carlos, 1999, Tese (doutorado) – Escola de Engenharia de São Carlos, Universidade de São Paulo, 123p.

[07] Marante, M. E., Flórez López, J. Three dimensional analysis of reinforced concrete frames based on Lumped Damage

Figure 11 – Flexural test set-up (21)

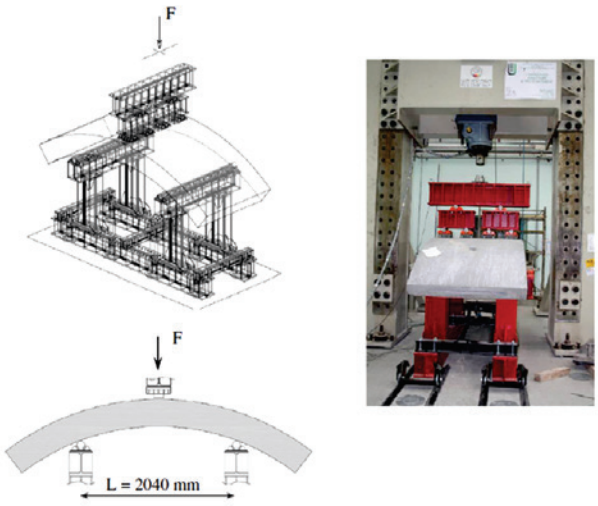

Figure 12 – Description of the problem

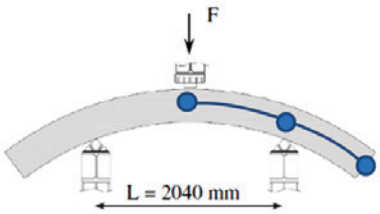

Figure 13 – Interaction diagrams

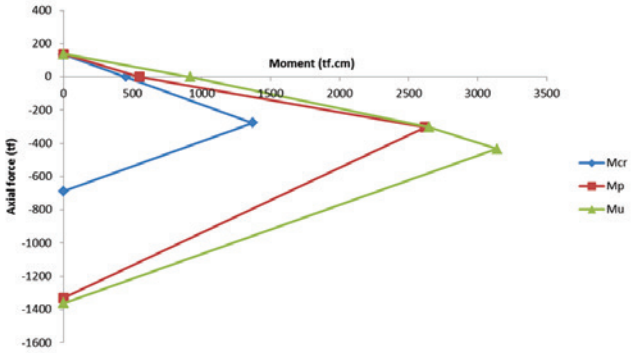

Figure 14 – Comparison between experimental and numerical responses

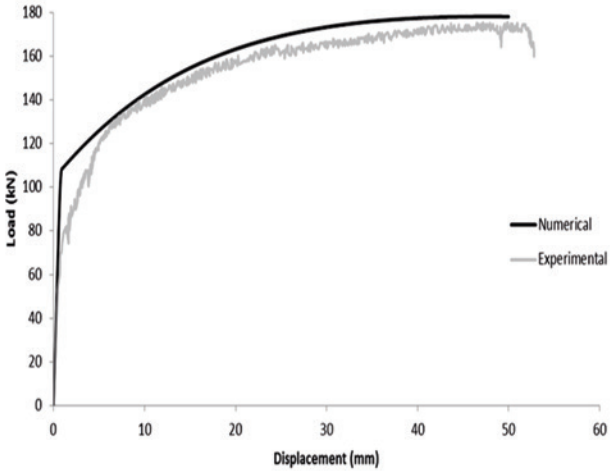

Figure 15 – Built tunnel in Osaka (a) using prestressed and precast concrete segments (b), (22)

Mechanics, International Journal of Solids and Structures, v.40, n.19, 2003; p.5109-5123.

[08] Alva, G. M. S. Estudo teórico-experimental do comportamento de nós de portico de concreto armado submetidos a ações cíclicas, São Carlos, 2004, Tese (doutorado) – Escola de Engenharia de São Carlos, Universidade de São Paulo, 218p.

Figure 16 – Flexural test set up (photo) (22)

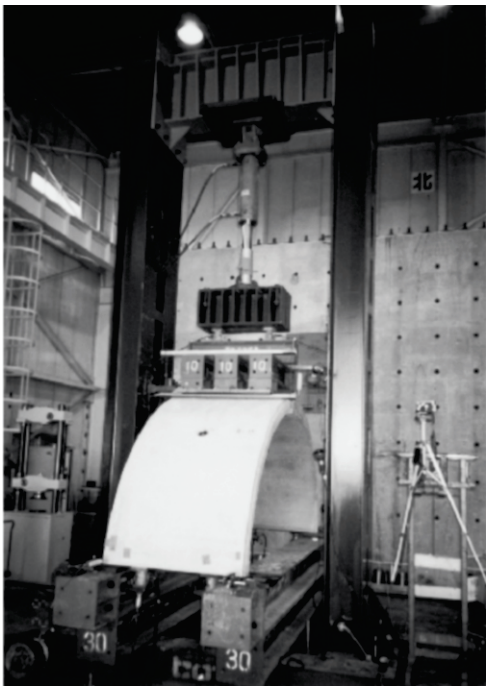

[09] Perdomo, M. E., Picón, R., Marante, M. E., Hild, F., Roux, S., Flórez-López, J. Experimental analysis and mathematical modeling of fracture in RC elements with any aspect ratio. Engineering Structures, n.46, 2013; p.407–416.

[10] Araújo, F. A., Proença, S. P. B. Application of a lumped dissipation model to reinforced concrete structures with the consideration of residual strains and cycles of hysteresis, Journal of Mechanics of Materials and Structures, v.3, n.5, 2008; p.1011-1031.

[11] Flórez-López J. Simplified model of unilateral damage for RC frames. Journal of Structural Engineering, v.121, n.12, 1995; p.1765–1772.

[12] Alva, G. M. S., El Debs, A. L. H. C., Application of lumped dissipation model in nonlinear analysis of reinforced concrete structures. Engineering Structures, v.32, n.4, 2010; p.974-981.

[13] Febres R, Inglessis P, Flórez-López J. Modeling of local buckling in tubular steel frames subjected to cyclic loading. Computers and Structures,v.81, 2003; p.2237–47.

[14] Palaninathan, R., Chandrasekharan, P. S. Curved beam element stiffness matrix formulation. Computers and Structures, v.21, 1985; p.663-669.

[15] Marquist, J. P., Wang, T. M. Stiffness matrix of parabolic beam element. Computers and Structures, v.31, 1989, p.863-870.

[16] Flórez-López, J., Proença, S. P. B. A curvilinear frame element with plastic hinges. *In*: IV International Symposium on Solid Mechanics, Porto Alegre, 2013.

[17] Tang, X. S., Zhang, J. R., Li, C. X., Xu, F. H., Pan, J. Damage analysis and numerical simulation for failure process of a reinforced concrete arch structure. Computers and Structures, v.83, 2005; p.2609-2631.

[18] Shi, Z. Crack analysis in structural concrete, theory and applications. Elsevier Oxford, 2009.

[19] Powell, H. G. Theory for nonlinear elastic structures. Journal of the Structural Division (ASCE), ST12, 1969; p.2687-2701.

[20] Avon, Z., Denis, T. Un algoritmo para mejorar la convergencia de problemas no lineales en mecánica de sólidos, Mérida,

Figure 17 – Flexural test set up (22)

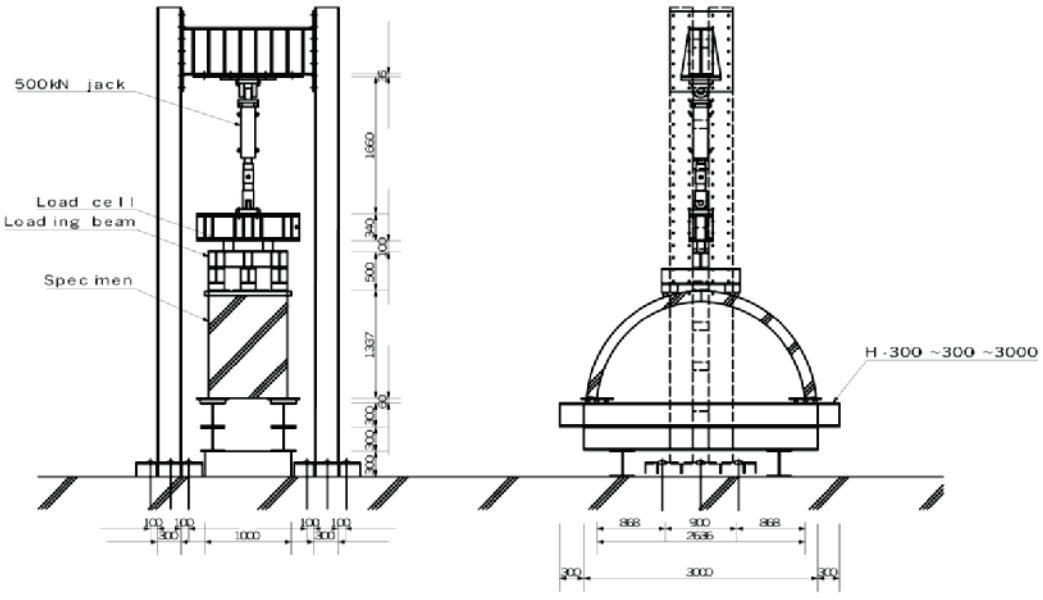

Figure 18 – Siplification of the problem

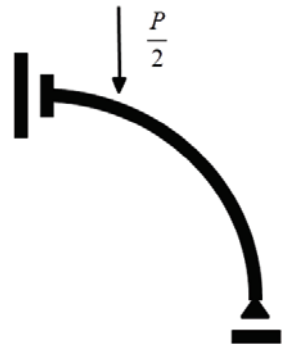

Figure 19 – Response to points of load application

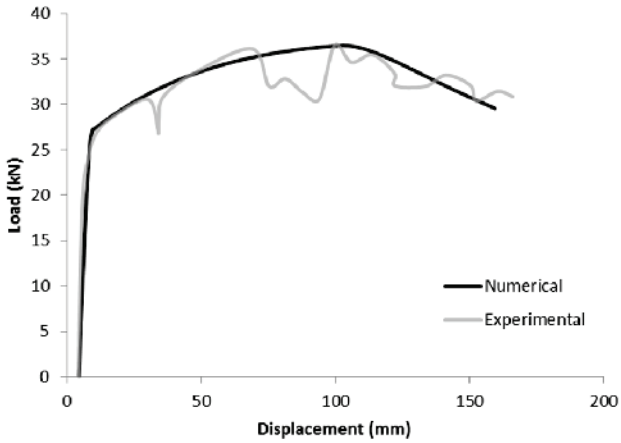

Figure 20 – Damage evolution on inelastic hinges

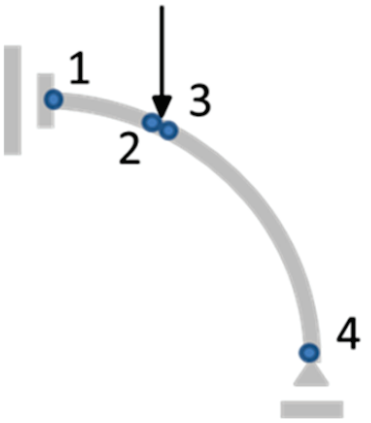

A

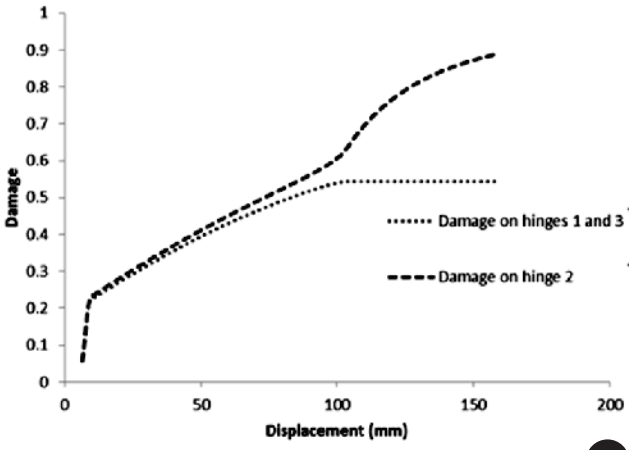

B

Figure 21 – Load and damage versus displacement

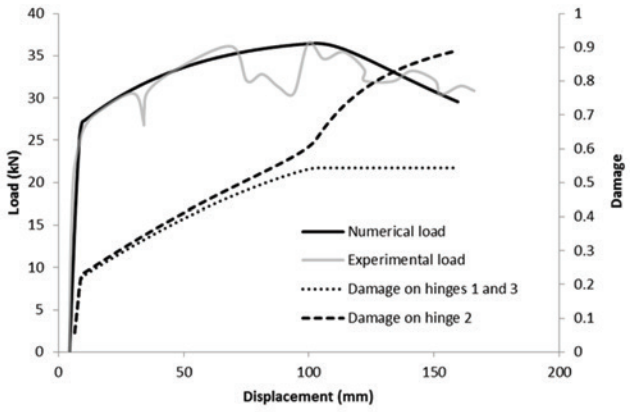

2002, Dissertação (mestrado) – Universidad de Los Andes.

[21] Caratelli, A., Meda, A., Rinaldi, Z., Romualdi, P. Structural behaviour of precast tunnel segments in fiber reinforced concrete. Tunnelling Underground and Space Technology, v.26, 2011; p.284-291.

[22] Nishikawa, K. Development of a prestressed and precast concrete segmental lining. Tunnelling Underground and Space Technology, v.18, 2003; p.243-251.

[23] Alarcón, E., Recuerdo, A., López, C., Gutierrez, J. P., de Diego, A., Picón, R., Flórez-López, J. A reparability index for reinforced concrete members based on fracture mechanics. Engineering Structures, v.23, n.6, 2001; p.687-697.

APPENDIX 1

Let (X_c, Z_c), (X_i, Z_i) and (X_j, Z_j) coordinates on the global axes of curvature of nodes *i* and *j* of a circular arch element. Worth then the relations:

$$(X_i - X_c)^2 - (Z_i - Z_c)^2 - R_b^2 = 0$$
$$(X_j - X_c)^2 - (Z_j - Z_c)^2 - R_b^2 = 0 \qquad (1)$$

Eliminating the value of radius in these expressions, it can isolate the value of X_c as a function of the other values:

$$X_c = \frac{X_i^2 + Z_i^2 - 2Z_iZ_c - X_j^2 - Z_j^2 + 2Z_jZ_c}{2(X_i - X_j)} \qquad (2)$$

The centre coordinate Z_c may be obtained by means of the resolution of the following equation: $aZ_c^2 + bZ_c + c = 0$; where:

$$a = \frac{Z_i^2 - 2Z_iZ_j - 2X_iX_j + Z_j^2 + X_i^2 + X_j^2}{(X_i - X_j)^2} \qquad b = -(X_i + X_j)a$$
$$c = X_i^2 - \frac{X_i(X_i^2 + Z_i^2 - X_j^2 - Z_j^2)}{(X_i - X_j)} + \frac{(X_i^2 + Z_i^2 - X_j^2 - Z_j^2)^2}{4(X_i - X_j)^2} + Z_i^2 - R_b^2 \qquad (3)$$

From equation (3) are obtained two different solutions to the centre coordinate. Particularly, if the nodes *i* and *j* are chosen clockwise and α is lower than π, then $\vec{ci} \times \vec{cj}$ is a vector in the positive direction of the global axis Y_G. This condition may be used to identify automatically the correct solution:

$$Z_iX_j - Z_iX_c - Z_cX_j - X_iZ_j + X_iZ_c + X_cZ_j > 0 \qquad (4)$$

Finally, the angles b_b and c_b are defined as:

$$\cos\beta_b = \frac{Z_i - Z_c}{R_b} \qquad \cos(\beta_b + \chi_b) = \frac{Z_j - Z_c}{R_b} \qquad (5)$$

APPENDIX 2

Consider again the circular element, now described in local coordinates (see figure 1). It is considered, next, a static variable defined by the vector of internal forces, however associated to the global coordinates: $\{\mathbf{Q}'\}_b^t = (Q'_{ui}, Q'_{wi}, Q'_{\theta i}, Q'_{uj}, Q'_{wj}, Q'_{\theta j})$.

$$n_i + Q'_{uj}\cos\chi_b + Q'_{wj}\sin\chi_b = 0 \qquad Q'_{wi} - Q'_{uj}\sin\chi_b + Q'_{wj}\cos\chi_b = 0 \qquad m_i + n_i R_b(1-\cos\chi_b) + R_b Q'_{wi}\sin\chi_b + m_j = 0 \tag{1}$$

In matrix form:

$$\{\mathbf{Q}'\}_b = [\mathbf{B}']_b^t \{\mathbf{M}\}_b \qquad [\mathbf{B}']_b = \begin{bmatrix} 0 & -\dfrac{1}{R_b\sin\chi_b} & 1 & -\dfrac{1}{R_b} & \dfrac{\cos\chi_b}{R_b\sin\chi_b} & 0 \\ 0 & -\dfrac{1}{R_b\sin\chi_b} & 0 & -\dfrac{1}{R_b} & \dfrac{\cos\chi_b}{R_b\sin\chi_b} & 1 \\ 1 & \dfrac{-1+\cos\chi_b}{\sin\chi_b} & 0 & -1 & \dfrac{-1+\cos\chi_b}{\sin\chi_b} & 0 \end{bmatrix} \tag{2}$$

The vectors of internal forces referenced by global coordinates, $\{\mathbf{Q}\}_b$, and local coordinates, $\{\mathbf{Q}'\}_b$, are related by means of the matrix of conventional geometric transformation $[\mathbf{T}]_b$:

$$\{\mathbf{Q}\}_b = [\mathbf{T}]_b \{\mathbf{Q}'\}_b \tag{3}$$

where $[\mathbf{T}]_b$ is defined as:

$$[\mathbf{T}]_b = \begin{bmatrix} \cos\beta_b & \sin\beta_b & 0 & 0 & 0 & 0 \\ -\sin\beta_b & \cos\beta_b & 0 & 0 & 0 & 0 \\ 0 & 0 & 1 & 0 & 0 & 0 \\ 0 & 0 & 0 & \cos(\chi_b+\beta_b) & \sin(\chi_b+\beta_b) & 0 \\ 0 & 0 & 0 & -\sin(\chi_b+\beta_b) & \cos(\chi_b+\beta_b) & 0 \\ 0 & 0 & 0 & 0 & 0 & 1 \end{bmatrix} \tag{4}$$

Figure 2.1 – Internal forces in local coordinates and generalised stresses

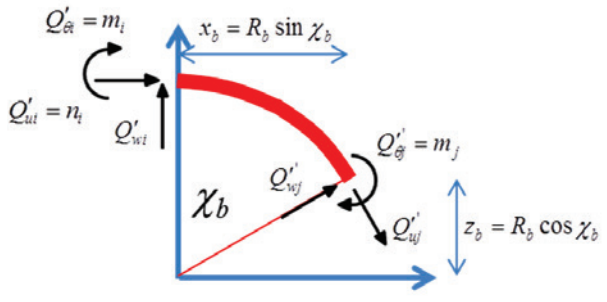

Therefore:

$$[\mathbf{B}]_b = [\mathbf{B}']_b [\mathbf{T}]'_b \tag{5}$$

The matrix of kinematic transformation to a straight element is obtained by means of an analogue procedure:

$$[\mathbf{B}]_b = \begin{bmatrix} \frac{\sin\alpha_b}{L_b} & -\frac{\cos\alpha_b}{L_b} & 1 & -\frac{\sin\alpha_b}{L_b} & \frac{\cos\alpha_b}{L_b} & 0 \\ \frac{\sin\alpha_b}{L_b} & -\frac{\cos\alpha_b}{L_b} & 0 & -\frac{\sin\alpha_b}{L_b} & \frac{\cos\alpha_b}{L_b} & 1 \\ -\cos\alpha_b & -\sin\alpha_b & 0 & \cos\alpha_b & \sin\alpha_b & 0 \end{bmatrix} \tag{6}$$

APPENDIX 3

Consider the circular element. Let $M(\theta)$, $V(\theta)$, and $N(\theta)$ the bending moment, shear force and axial force in a cross-section identified by an angle θ from the edge *i* (see figure 1).
The equilibrium relations are, now, written as:

$$\begin{aligned} & n_i + N(\theta)\cos\theta - V(\theta)\sin\theta = 0 \\ & Q'_{wi} - N(\theta)\sin\theta - V(\theta)\cos\theta = 0 \\ & m_i + n\,R(1-\cos\theta) + R\,Q'_{wi}\,\sin\theta - M(\theta) = 0 \end{aligned} \tag{1}$$

The system of equations (1) associated to the expression of internal force Q'_{wi} obtained in appendix 2 allows express the axial force, shear force and bending moment in terms of the generalised stresses:

$$\begin{aligned} M(\theta) &= -\frac{-m_i\sin\chi_b - n_i R_b\sin\chi_b + n_i R_b\cos\theta\sin\chi_b + m_i\sin\theta_b + n_i R_b\sin\theta_b - n_i R_b\sin\theta\cos\chi_b + m_j\sin\theta}{\sin\chi_b} \\ V(\theta) &= \frac{-m_i\cos\theta - n_i R_b\cos\theta + n_i R_b\cos\theta\cos\chi_b - m_j\cos\theta + n_i R_b\sin\chi_b\sin\theta}{R_b\sin\chi_b} \\ N(\theta) &= -\frac{m_i\sin\theta + n_i R_b\sin\theta - n_i R_b\sin\theta\cos\chi_b + m_j\sin\theta + n_i R_b\sin\chi_b\cos\theta}{R_b\sin\chi_b} \end{aligned} \tag{2}$$

The elastic strain energy in the element may then be written as:

$$U_b = \int_0^{\chi_b}\left(\frac{M(\theta)^2}{2EI_b} + \frac{N(\theta)^2}{2AE_b} + \frac{V(\theta)^2}{2GA_b}\right)R_b\,d\theta \tag{3}$$

Figure 3.1 – Axial force, bending moment and shear force on the circular element

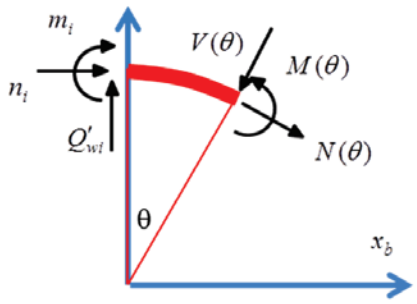

where the terms EI_b, GA_b and AE_b have the usual meaning. The coefficients of the elastic flexibility matrix may be obtained from the Castigliano's theorem. Particularly, if the shear deformations are neglected those coefficients are:

$$F_{11}^0 = \frac{\partial^2 U_b}{\partial m_i \partial m_i} = \frac{1}{4}\frac{R_b\left(-8\sin\chi_b + 6\chi_b - 4\chi_b\cos^2\chi_b + 6\sin\chi_b\cos\chi_b\right)}{EI_b\sin^2\chi_b} - \frac{1}{4}\frac{2\sin\chi_b\cos\chi_b - 2\chi_b}{R_b AE_b\sin^2\chi_b}$$

$$F_{12}^0 = \frac{\partial^2 U_b}{\partial m_i \partial m_j} = \frac{1}{4}\frac{R_b\left(-4\sin\chi_b + 2\chi_b + 2\sin\chi_b\cos\chi_b\right)}{EI_b\sin^2\chi_b} - \frac{1}{4}\frac{2\sin\chi_b\cos\chi_b - 2\chi_b}{R_b AE_b\sin^2\chi_b}$$

$$F_{13}^0 = \frac{\partial^2 U_b}{\partial m_i \partial n_i} = \frac{1}{4}\frac{R_b\left(-10R_b\sin\chi_b + 10\sin\chi_b R_b\cos\chi_b - 2R_b\chi_b\cos\chi_b - 6R_b\chi_b - 4R_b\chi_b\cos^2\chi_b\right)}{EI_b\sin^2\chi_b}$$
$$- \frac{1}{4}\frac{-2R_b\sin\chi_b - 2R_b\chi_b + 2\sin\chi_b R_b\cos\chi_b + 2\chi_b R_b\cos\chi_b}{R_b AE_b\sin^2\chi_b}$$

$$F_{22}^0 = \frac{\partial^2 U_b}{\partial m_j \partial m_j} = \frac{1}{4}\frac{R_b\left(2\chi_b - 2\sin\chi_b\cos\chi_b\right)}{EI_b\sin^2\chi_b} - \frac{1}{4}\frac{2\sin\chi_b\cos\chi_b - 2\chi_b}{R_b AE_b\sin^2\chi_b}$$

$$F_{23}^0 = \frac{\partial^2 U_b}{\partial m_j \partial n_i} = \frac{1}{4}\frac{R_b\left(-2R_b\sin\chi_b - 2R_b\chi_b\cos\chi_b + 2R_b\chi_b + 2\sin\chi_b R_b\cos\chi_b\right)}{EI_b\sin^2\chi_b}$$
$$- \frac{1}{4}\frac{-2R_b\sin\chi_b - 2R_b\chi_b + 2\sin\chi_b R_b\cos\chi_b + 2\chi_b R_b\cos\chi_b}{R_b AE_b\sin^2\chi_b}$$

$$F_{33}^0 = \frac{\partial^2 U_b}{\partial n_i \partial n_i} = \frac{1}{4}\frac{R_b\left(-12R_b^2\sin\chi_b + 12\sin\chi_b R_b^2\cos\chi_b - 4R_b^2\chi_b\cos^2\chi_b - 4R_b^2\chi_b\cos\chi_b + 8R_b^2\chi_b\right)}{EI_b\sin^2\chi_b}$$
$$- \frac{1}{4}\frac{-4R_b^2\sin\chi_b + 4\sin\chi_b R_b^2\cos\chi_b - 4R_b^2\chi_b + 4\chi_b R_b^2\cos\chi_b}{R_b AE_b\sin^2\chi_b}$$

(4)

The elastic flexibility matrix to a straight element is obtained by an analogue procedure, resulting:

$$[\mathbf{F}_0] = \begin{bmatrix} \frac{L_b}{3EI_b} & -\frac{L_b}{6EI_b} & 0 \\ -\frac{L_b}{6EI_b} & \frac{L_b}{3EI_b} & 0 \\ 0 & 0 & \frac{L_b}{AE_b} \end{bmatrix}$$

(5)